Synthesis and Initial Evaluation of 17-^{11}C-Heptadecanoic Acid for Measurement of Myocardial Fatty Acid Metabolism

T. Lee Collier, PhD[1,2]; Yuying Hwang, PhD[1]; Ravichandran Ramasamy, PhD[1]; Robert R. Sciacca, EngScD[1]; Kathleen T. Hickey, EdD[1]; Norman R. Simpson, BS[2]; and Steven R. Bergmann, MD, PhD[1,2]

[1]Division of Cardiology, Department of Medicine, College of Physicians and Surgeons of Columbia University, New York, New York; and [2]Department of Radiology, College of Physicians and Surgeons of Columbia University, New York, New York

Fatty acid oxidation defects are being increasingly identified as causes of abnormal heart function and sudden death in children. Children with medium-chain acyl-coenzyme A (acyl-CoA) dehydrogenase defects can metabolize fatty acids labeled in the carboxylic acid end of the compound. Accordingly, our goal was to label a long-chain fatty acid in the ω-position and evaluate its myocardial kinetics. **Methods:** Heptadecanoic acid, a 17-carbon fatty acid, was labeled in the C-17 position with ^{11}C by the general process of coupling ^{11}C-methyliodide to *t*-butyl-15-hexadecanoate. Yield was ~5%–10% end-of-bombardment. Subsequently, evaluation studies were performed on isolated perfused rat hearts and in intact, anesthetized dogs. The myocardial uptake and efflux of 17-^{11}C-heptadecanoic acid were compared with those of 1-^{11}C-palmitate. **Results:** With the exception of delayed efflux of tracer reflecting the temporal delay for β-oxidation, the washout of 17-^{11}C-heptadecanoic acid from the heart mirrored that of 1-^{11}C-palmitate in isolated rat hearts and in intact dogs with PET. **Conclusion:** 17-^{11}C-Heptadecanoic acid may be a useful tracer for the identification of defects in fatty acid metabolism in subjects with medium- and short-chain fatty acid oxidation defects.

Key Words: fatty acid metabolism; inherited defects; fatty acid oxidation disorders; myocardial metabolism

J Nucl Med 2002; 43:1707–1714

Fatty acid oxidation defects are increasingly recognized inherited deficiencies in which specific organs are unable to oxidize fatty acid for energy because a critical enzyme is either missing or not working correctly. These defects can have a profound impact on the heart because the heart preferentially uses long-chain fatty acids for energy production (*1–4*).

We have shown previously that children with long-chain, very-long-chain, or 3-hydroxy acyl-coenzyme A (acyl-CoA) dehydrogenase deficiency (inherited disorders in which the heart is unable to efficiently break down long-chain fatty acid through the β-oxidation pathway) can be identified with 1-^{11}C-palmitate (*5*). This finding is based on the fact that, in these individuals, the deficient enzyme is needed in the initial step of β-oxidation in which a 2-carbon fragment is broken off from the carboxylic side of the fatty acid in the first cycle of β-oxidation. In these children, fatty acids are taken into the heart relatively normally, but oxidation is diminished and long-chain fatty acids are shunted to a slow-turnover pool predominantly representing incorporation of long-chain fatty acids into triglycerides.

However, 1-^{11}C-palmitate cannot be used to interrogate patients with medium-chain or short-chain acyl-CoA-dehydrogenase (MCAD and SCAD, respectively) deficiencies because, in these individuals, the enzyme defect enables initial β-oxidation of long-chain fatty acids but prevents complete β-oxidation when the fatty acid reaches 6–12 carbons long (in the case of MCAD) or 4–6 carbons long (in the case of SCAD). This is because specific acyl-CoA dehydrogenases are required for different chain lengths of fatty acids.

MCAD deficiency is thought to be the most common defect of mitochondrial β-oxidation in humans (*6*). It is an autosomal recessive disorder that usually presents in infancy and manifests itself in periods of metabolic stress. SCAD is uncommon and is usually asymptomatic. To better identify abnormalities in fatty acid oxidation in children with these disorders, a long-chain fatty acid labeled in the ω-side of the fatty acid is needed. Although short- and medium-chain fatty acids can be labeled in the C-1 carboxylic acid position, their extraction by the myocardium is minimal, thereby resulting in a negligible myocardial-to-blood signal.

We showed previously that palmitate, a 16-carbon long-chain fatty acid, which is abundant in arterial blood and which is avidly used by the myocardium, could be labeled in the C-16 position (*7*). However, labeling in this position results in a C-2 label when the fatty acid is broken down by β-oxidation. Because the C-2 carbon does not immediately

Received Jan. 24, 2002; revision accepted Jul. 26, 2002.

For correspondence or reprints contact: T. Lee Collier, PhD, Division of Cardiology, VC 12-238, College of Physicians and Surgeons of Columbia University, 630 W. 168th St., New York, NY 10032.

E-mail: tc311@columbia.edu

proceed to oxidation, the results of efflux are not directly related to β-oxidation. Accordingly, a long-chain fatty acid labeled in the penultimate position (i.e., labeled in the C-15 position for a 16-carbon fatty acid such as palmitate) would be ideal, but this has been difficult to accomplish.

An alternative strategy is to label an odd-chain-length fatty acid in the ω-position. We chose the 17-carbon heptadecanoic acid (17-^{11}C-HDA) for this purpose. β-Oxidation of 1-^{11}C- or [ω-1]-^{11}C-palmitate results in 1-^{11}C-acetate after β-oxidation. Odd-numbered fatty acids, however, are metabolized by β-oxidation to a 3-carbon propionyl group. Propionyl CoA can be used by the heart and is capable of entering the tricarboxylic acid cycle. Accordingly, the objectives of this study were to synthesize and analyze the kinetics of 17-^{11}C-HDA in comparison with that of 1-^{11}C-palmitate to determine whether the ω-labeled fatty acid would enable assessment of β-oxidation.

MATERIALS AND METHODS

All studies were performed under approved animal protocols of the Institutional Animal Care and Use Committee of Columbia University.

Isolated Perfused Rat Hearts

Isolated perfused hearts were initially evaluated because they permit precise control of myocardial perfusion and loading. Studies were performed, under constant flow maintained by a roller pump, using an isolated heart preparation as described from our laboratory (*8*), on 2 hearts. Briefly, rats were anesthetized using a mixture of ketamine and xylazine (80 and 10 mg/kg, respectively, administered intraperitoneally). After a deep anesthesia, hearts were rapidly excised, placed into iced saline, and perfused retrogradely at 37°C in a nonrecirculating mode. The hearts were perfused with a modified Krebs–Henseleit buffer containing 5 mmol/L glucose and 0.4 mmol/L palmitate complexed to equimolar bovine serum albumin and 70 mU/L of insulin. The perfusate was equilibrated with a mixture of 95% oxygen and 5% CO_2 that maintained the perfusate partial pressure of oxygen at >600 mm Hg. All hearts were paced at 300 beats per minute and stabilized for 30 min before administration of tracers.

All tracers were injected using as small a volume as possible (<100 μL) and injected as a bolus over ~10 s. All injections of the tracers were made in triplicate for each heart and were made after allowing sufficient time for the activity in the hearts to return to baseline from the previous injection. Data were collected using a detector system placed across the heart as described (*8*). 1-^{11}C-Palmitate and 17-^{11}C-HDA (~300 kBq) were administered in randomized order. Time–activity data were collected for 20 min at 1 sample per second in both the coincidence and singles mode, corrected for decay, and normalized to the peak uptake. Curves were fitted with a biexponential function. Hemodynamics and myocardial metabolism were monitored as described (*8,9*). Comparisons were made between uptake efflux of radioactivity after administration of 1-^{11}C-palmitate and 17-^{11}C-HDA.

Canine Studies

To evaluate the uptake of 17-^{11}C-HDA in an intact animal model, 3 adult conditioned dogs weighing ~25 kg each were fasted overnight, sedated with morphine sulfate (2 mg/kg subcutaneously), and then anesthetized with thiopental (12.5 mg/kg, subcutaneously) and α-chloralose (72 mg/kg, intravenously). Dogs were then intubated and ventilated with room air, and additional α-chloralose was administered as necessary to maintain a stable level of anesthesia. Catheters were placed in the thoracic aorta via the femoral artery for arterial blood sampling. A femoral vein was catheterized for administration of drugs. Then, under fluoroscopic guidance, a catheter was placed retrogradely in the left atrium via the aorta for the administration of colored microspheres to measure myocardial blood flow and perfusion (*10,11*). Another catheter was advanced 1–4 cm into the coronary sinus from the right jugular vein for direct coronary sinus sampling of metabolites. After catheterization was completed, dogs received 5,000 units of heparin intravenously, which was repeated every 90 min. Two dogs were studied under baseline conditions with no further intervention. One dog was treated with a constant infusion of dobutamine at 10 μg/kg·min to increase myocardial contraction and thus metabolism.

After stabilization, animals were transported to the PET scanner and again allowed to stabilize. Myocardial perfusion was measured with colored microspheres (*10,11*). Then, after administration of either 1-^{11}C-palmitate or 17-^{11}C-HDA, paired blood samples were obtained from the arterial and coronary sinus catheters at 1, 5, 10, and 20 min. These samples were obtained for measurement of ^{11}C-CO_2, which is the result of oxidation, and for determination of metabolites.

All animals were studied on an ECAT EXACT 47 (CTI, Knoxville, TN) that provides simultaneous acquisition of 47 transaxial planes. The performance characteristics of this scanner have been reported (*12*). Using the filters in our laboratory, the reconstructed resolution is ~1.2 cm in plane. A short scan was obtained using the ^{68}Ge/^{68}Ga rod source for correct positioning and then a 10-min transmission scan was obtained. 1-^{11}C-Palmitate (~185 MBq [~5 mCi]) was administered as a bolus, and data were collected for a total of 29 min (18 × 5-s frames, followed by 10 × 30-s frames, followed by 15 × 60-s frames, and followed by 3 × 2.5-min frames). After allowing ~60 min, after imaging, for decay of the 1-^{11}C-palmitate, 17-^{11}C-HDA (~37–78 MBq [~1–2 mCi]), prepared as described below, was administered as an intravenous bolus, and data were collected analogously to that for 1-^{11}C-palmitate.

Analysis of PET Images

Data from the 47 transaxial planes in each scan were decay corrected and reoriented into the true short- and long-axis slices. Regions of interest were defined in 4 standard equal segments in each short-axis reconstruction, and in 5 standard regions in each of the horizontal and vertical long-axis reconstructions. In addition, a small region of interest was defined in each of the most basal short-axis reconstructions for delineation of the arterial input curve.

Arterial curves were corrected for metabolites from the timed arterial samples that were collected after administration of tracer (see below). Then, blood and tissue time–activity curves were entered into a multicompartmental model that defines the rate of uptake of fatty acid, as described (*5,13*).

Blood Analysis

At the beginning and end of each metabolic scan, paired arterial and coronary sinus samples were obtained for assay of fatty acids, glucose, and lactate. Steady-state myocardial fatty acid, glucose, lactate, and oxygen utilization were calculated from the arterial −

coronary sinus difference for each substance multiplied by myocardial blood flow as assessed with colored microspheres (*10,11*). For metabolic analyses, blood was placed in heparinized tubes, immediately placed on ice, and centrifuged rapidly at 4°C. Plasma was separated and frozen at −70°C until assay. Individual fatty acids were measured by gas chromatography (GC), and glucose and lactate were assayed enzymatically as described (*13*).

To correct the arterial input for metabolism of tracers to ^{11}C-CO_2, timed arterial and coronary sinus samples were collected and processed as described (*13*). Briefly, total ^{11}C radioactivity was measured in blood contained in vials containing 70% isopropyl alcohol and 0.1N sodium hydroxide. Non–^{11}C-CO_2 radioactivity was measured in tubes containing 70% isopropyl alcohol and 5.5% sodium bicarbonate. This tube was then acidified with 1 mL 6N hydrochloric acid and bubbled with nitrogen for 10 min to release ^{11}C-CO_2. All results were normalized for weight of blood.

To determine the breakdown of 17-^{11}C-HDA after administration, arterial blood samples (1 mL) were taken at 1 and 10 min after administration of 17-^{11}C-HDA. After centrifugation of the whole blood, the supernate and precipitate were counted by well scintigraphy to determine radioactivity in each fraction. The supernate was then treated with 100 μL each of 2 mg/mL glutamic acid, 2 mg/mL propionic acid, and 2 mg/mL HDA followed by 1 mL acetonitrile to precipitate proteins. The samples were then centrifuged. After centrifugation, both the supernate and the precipitate were counted by well scintigraphy to determine radioactivity associated with the proteins. The entire supernate was applied to a 20 × 20 cm, 0.25-mm polystyrene-backed silica gel plate. The plate was developed to ~1 cm from the top of the plate in a solution of chloroform:methanol:water:ammonium hydroxide (4:6:1:0.1). Plates were removed from the solvent and the distance from the origin to the solvent front was divided into 10 horizontal bands of equal size. Each band was placed into scintillation vials with the remaining top portion of the plates placed into a separate vial to determine background radioactivity. The regions corresponding to HDA ($R_f \approx 0.7–0.8$), glutamate or aspartate (under these conditions, both yielded a similar $R_f \approx 0.5$), and propionic acid ($R_f \approx 0.2$) were combined from the thin-layer chromatographic (TLC) plate, and the percentage activity contained in each of the regions was determined from each blood sample.

Synthesis of Tracers

1-^{11}C-Palmitate was prepared as described (*14*). The general synthesis for the 17-^{11}C-HDA is shown in Figure 1 and followed the general synthesis method described for 16-^{11}C-palmitic acid (*15*). Proton nuclear magnetic resonance (NMR) spectra were

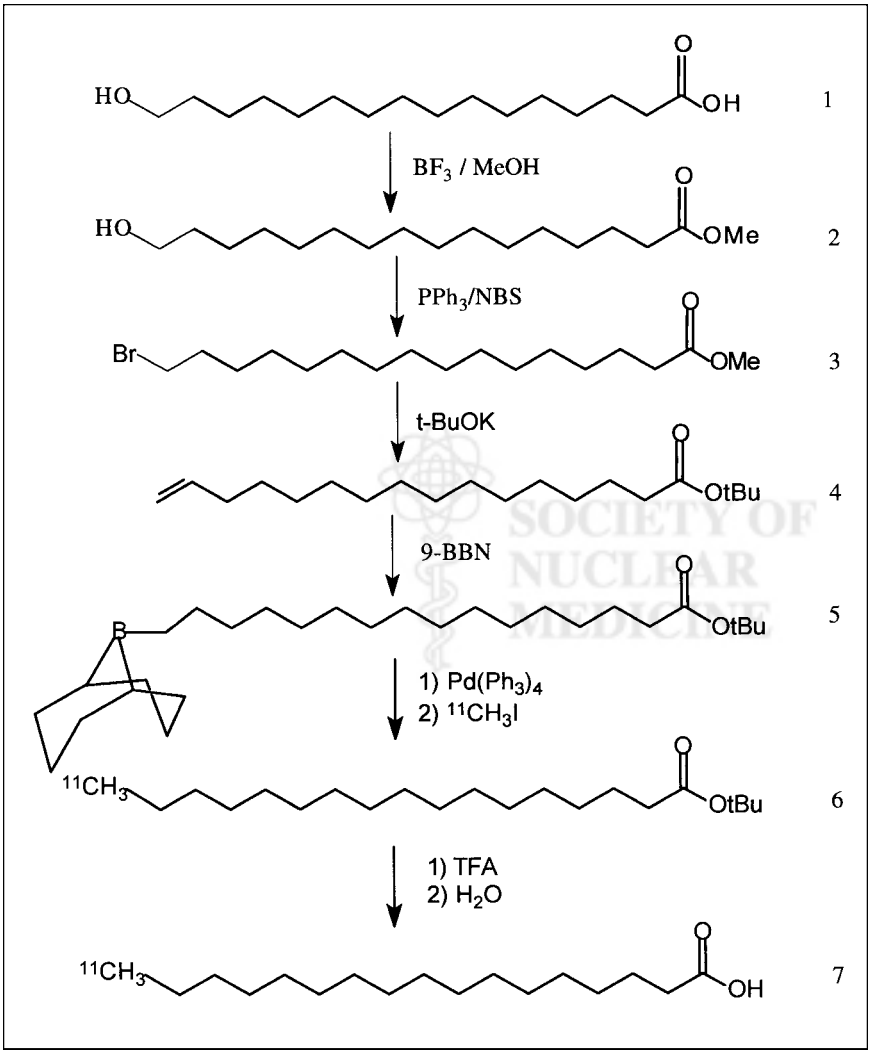

FIGURE 1. Synthesis and radiosynthesis of 17-^{11}C-HDA. PPh_3 = triphenylphosphine; NBS = *N*-bromosuccinimide; 9-BBN = 9-borabicyclo[3.3.1]nonane; $Pd(Ph_3)_4$ = tetrakis(triphenylphosphine)palladium(0); TFA = trifluoroacetic acid.

recorded on a JEOL 400-MHz FT-NMR spectrometer (Peabody, MA). Chemical shifts were recorded in ppm (δ) from an internal tetramethylsilane standard in deuterochloroform and coupling constants (J) are reported in Hz. Melting points were recorded on a MEL-TEMP II (Laboratory Devices Inc., Holliston, MA) melting point apparatus and are uncorrected. Elemental analysis was performed by Atlantic Microlab (Norcross, GA). Gravity chromatography was performed using silica gel (70–230 mesh; Aldrich, Milwaukee, WI) with the solvent systems indicated in the text. For mixed solvent systems, the ratios are given with respect to volumes.

All reagents were purchased from commercial sources and were used without further purification, except for the tetrahydrofuran (THF), which was distilled over sodium and benzophenone under an argon atmosphere. ^{11}C-CO_2 was obtained from the Kreitchman Medical Cyclotron (RDS-112; CTI Inc., Knoxville, TN). Radiochemical yields are based on the amount of ^{11}C-CO_2 delivered to the hot cell. High-performance liquid chromatographic (HPLC) analysis of the radioligand was performed using a Millennium Data Acquisition System (Waters, Milford, MA), a 515 HPLC pump (Waters), a Bioscan Flow Count Radiation Detector system (Bioscan, Inc., Washington, DC), and 1 of the following detectors: a Rainin Dynacomp Absorbance Detector model UV-C (Rainin Instrument Co., Woburn, MA), a Shodex RI-71 Refractive Index detector (Shodex, Showa, Denko, K.K., Japan), or a 776 PDA detector (Waters). The HPLC columns used were C18-LL, 5 μm, 10 × 100 mm (Alltech Associates, Deerfield, IL), for the semipreparative separation. Analytic analysis of the final product was performed using a Prodigy Phenomenex (Phenomenex, Torrance, CA), C8, 10 μm, 4.6 × 250 mm, and a mobile phase of methanol and 1.7 mol/L acetic acid (90:10). GC analysis was performed using a 5890A gas chromatograph (Hewlett-Packard Co., Palo Alto, CA) and a NUKOL (30 m × 0.53 mm, 0.2-μm film thickness; Supelco, Bellefonte, PA), with the instrument temperatures as reported in the experimental section. Chemical and radiochemical purity of the radiotracer was performed on the ethanol solution, before formulation in albumin.

Methyl-16-Hydroxyhexadecanoate, **2**. To a stirred solution of 16-hydroxyhexadecanoic acid, **1** (1 g, 3.6 mmol), in 40 mL anhydrous methanol, was added 50% boron trifluoride in methanol (6.5 mL), and the reaction mixture was stirred at room temperature for 1 min. The reaction vessel was then heated at reflux for 5 min and allowed to cool to room temperature. The reaction mixture was transferred to a 250-mL separatory funnel and diluted with ~100 mL chloroform and shaken. Then the organic layer was washed with ~100 mL deionized water. The aqueous layer was extracted with 2 × 100 mL chloroform, the combined organic layers were dried over sodium sulfate, and the solvent was removed in vacuo. The crude product was recrystallized 3 times from hexane to yield 0.80 g (76%), a colorless solid, purity >99% by GC (190°C): mp 51°C–52°C; ^1H NMR: δ 1.2–1.4 (bs, 22H), 1.58 (m, 2H), 1.6 (m, 2H), 2.32 (t, 2H, J = 7 Hz), 3.65 (t, 2H, J = 7 Hz), 3.68 (s, 3H).

Methyl 16-Bromohexadecanoate, **3**. To a stirred solution of alcohol, **2** (2.7 g, 9.44 mmol), and triphenylphosphine (2.89 g, 10.4 mmol, 1.1 equivalence) in 20 mL dimethylformamide was added *N*-bromosuccinimide (NBS) (3.91 g, 21.9 mmol, 2.3 equivalence) in portions. After the addition of the NBS was complete, the reaction was stirred at room temperature for 10 min, under nitrogen, and then heated at 55°C for 30 min. The reaction was allowed to cool to room temperature, and then 20 mL of methanol were added followed by 1N HCl (200 mL). The reaction was worked up with ether and, after drying the organic layer and concentrating the product in vacuo, a pink-colored solid was obtained. The solid was triturated with hexane to dissolve the product and leave the triphenylphosphine oxide behind. Flask chromatography on silica gel (20:1 hexanes:ethyl acetate) afforded 2.46 g (75%) of pure bromide (>98% by GC): mp 33°C–35°C; ^1H NMR: δ = 1.1–1.38 (m, 24H), 1.4 (m, 2H), 1.8 (m, 2H), 2.3 (t, 2H, J = 7), 3.69 (s, 3H).

t-*Butyl-15-Hexadecanoate,* **4**. To a 1.0 mol/L solution of *t*-BuOK in THF (15 mL) was added **3** (1.59 g, 4.56 mmol). After the solution was stirred at room temperature for 1 h, 1N HCl (150 mL) was added to the brown-colored solution and the reaction mixture was stirred for 5 min. The reaction mixture was worked up with ether to afford the alkene, **4**. Flash chromatography on silica gel (hexane) gave 1.7 g (70%) of pure **4** as a colorless oil. ^1H NMR: δ = 1.20–1.35 (bs, 20H), 1.37 (m, 2H), 1.46 (s, 9H), 2.06 (m, 2H), 2.3 (t, 2H, J = 7), 4.90 (ddt, 2H), 4.97 (ddt, 1H), 5.80 (ddt, 1H).

^{11}C-Methyl Iodide. ^{11}C-CO_2 was produced by the $^{14}N(p,\alpha)^{11}C$ nuclear reaction and was converted to ^{11}C-CH_3I following the general method of Långström et al. (*16*).

Preparation of t-*Butyl-15-Hexadecanoate–Borane Complex,* **5**. To a 1-mL dry Wheaton vial, was added 10 mg *t*-butyl-15-hexadecanoate, **4** (33 μmol), and this was dissolved in 1 mL anhydrous THF. To the stirred solution was added a slight excess of 9-borabicyclo[3.3.1]nonane (9-BBN) (75 μL, 0.5 mol/L in THF, 1.1 equivalent) and the solution was allowed to stir at room temperature for 30 min. The borane complex was not purified before subsequent use. The solution was stable at room temperature for several days.

17-^{11}C-HDA, **7**. Five hundred microliters (~15 μmol) of the borane stock solution were added to a clean dry 1-mL Wheaton vial, and the ^{11}C-CH_3I (17 GBq [463 mCi]) was collected in the vial at room temperature. Then the vial was assayed before continuation of the reaction. An ~100-μL aliquot of an anhydrous THF solution of tetrakis(triphenylphosphine)palladium(0) (4–12 mg/mL) and ~10 μL of aqueous sodium hydroxide (5 mol/L, 3 equivalents relative to the borane complex) were injected into the vial. The resulting solution was heated at 90°C for 5 min. The reaction vessel was removed from the heat and cooled for ~1 min in a water bath; then a sweep of inert gas was applied to the vial to remove any volatile gases and trap them in a gas bag for decay. The reaction mixture was then applied to a dry 1 × 8 cm column of silica gel and the ester, **6**, was eluted off the column with 5 mL diethyl ether directly into a 5-mL Wheaton vial with a gas trap attached. The ether was removed under a stream of inert gas; then 1 mL trifluoroacetic acid was added to the 5-mL flask and the flask was heated at 90°C for 2 min. The flask was removed from the heat and quickly cooled in a water bath; then 1 mL deionized water and 1 mL diethyl ether were added and the reaction vessel was shaken for 1 min to extract the free fatty acid. The ether layer was transferred to a reaction vial containing 1 mL ethanol and the ether was quickly removed under a stream of inert gas. The remaining ethanol solution was diluted with the HPLC mobile phase and was injected onto a 1 × 10 cm HPLC column (ethanol:17 mmol/L acetic acid, 65:35; 4 mL/min). The desired compound was collected at a retention time of 9–12 min, and the product was extracted with two 10-mL aliquots of petroleum ether. The petroleum ether extracts were combined with 1 mL ethanol and the petroleum ether was removed under a stream of inert gas until a volume of slightly <1 mL remained. An aliquot of the ethanol solution was removed for the determination of chemical and radiochemical purity and the remaining solution was then diluted

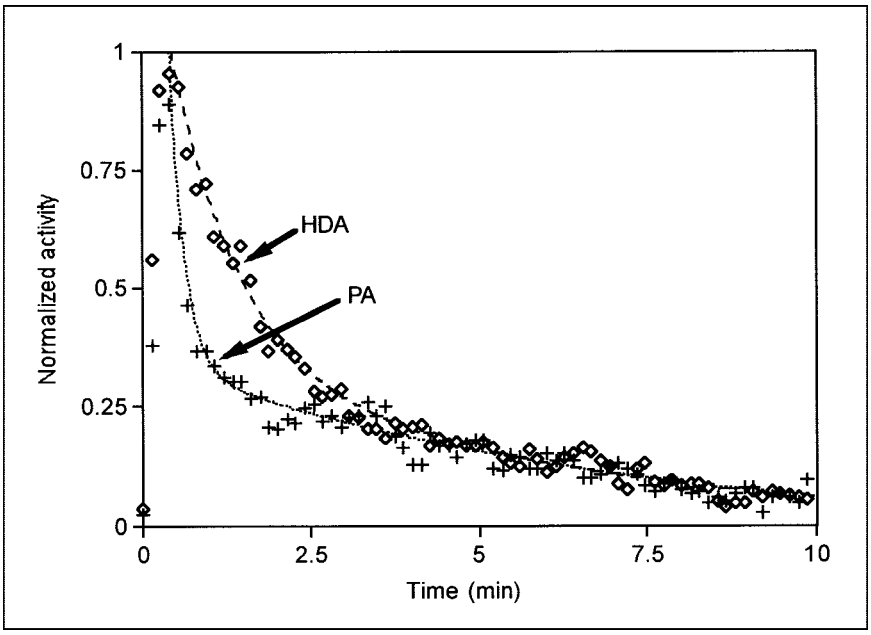

FIGURE 2. Time–activity curves from isolated perfused heart, injected with 1-^{11}C-palmitate (PA) and 17-^{11}C-HDA. Biexponential curves were fit by simplex method using Excel (Microsoft, Redmond, WA). Analysis of curves indicates that rates for rapid early clearance are significantly different for the 2 tracers, -5.861 ± 0.14 vs. -1.281 ± 0.11 min^{-1} (PA and HDA, respectively); however, slow-clearance portion showed no significant difference, -0.318 ± 0.007 vs. -0.300 ± 0.024 min^{-1} (PA and HDA, respectively).

with ~9 mL 3.5% albumin in saline (maintained at 40°C). The albumin solution was filtered, while warm, through a 0.22-μm sterile filter into a sterile vial to yield 290 MBq (7.8 mCi) of product. The radiochemical yield of the reaction typically was 5%–10% end-of-bombardment (EOB) from ^{11}C-CO_2.

RESULTS

Isolated Perfused Hearts

Isolated perfused heart studies were conducted on 2 isolated hearts to examine the kinetics of terminally labeled 17-^{11}C-HDA compared with that of 1-^{11}C-palmitate. All studies were performed using nonrecirculating media so results would not be confounded by metabolites recirculating back to the heart.

Time–activity curves from 1 such experiment are shown in Figure 2, which has been corrected for decay and normalized to the peak tracer activity. From Figure 2, it is clear that the rates for the early rapid portion of clearance of the tracer are significantly different for the 2 tracers, -5.861 ± 0.14 min^{-1} compared with -1.281 ± 0.11 min^{-1} for 1-^{11}C-palmitate and 17-^{11}C-HDA, respectively. However, the slower portion of clearance showed no significant difference (-0.318 ± 0.007 and -0.30 ± 0.024 min^{-1}) for 1-^{11}C-palmitate and 17-^{11}C-HDA, respectively. These data suggest that, although there is a slight delay in the initial processing (i.e., β-oxidation) of HDA, once it is broken down to the 3-carbon propionate species, it clears the heart at a rate similar to that of 1-^{11}C-palmitate.

PET

High-quality images of the myocardium were obtained using both 1-^{11}C-palmitate and 17-^{11}C-HDA. Of note, the quality of the 17-^{11}C-HDA images was similar to that of 1-^{11}C-palmitate despite using ~20% of the administered activity (Fig. 3).

Time–activity curves were obtained from multiple regions of interest in the left ventricular wall. After correction for activity and the weight of the animal, as demonstrated in Figure 4, more HDA was extracted by the myocardium compared with 1-^{11}C-palmitate.

Three dogs were studied, 2 under basal conditions and 1 during infusion of 10 μg/kg·min dobutamine. As shown in Table 1, steady-state palmitate utilization increased with dobutamine as expected. Modeled palmitate utilization is shown in Table 2. Fatty acid utilization estimated with a compartmental model correlated well with utilization measured directly. The directly determined fatty acid extraction

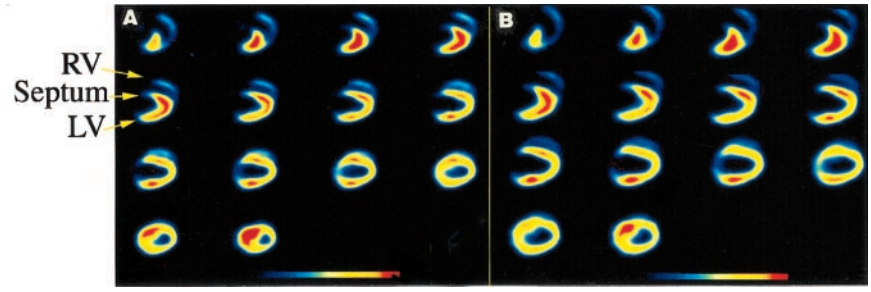

FIGURE 3. Tomographic reconstructions from control dog injected with 185 MBq (5 mCi) 1-^{11}C-palmitate (PA) (A) and injected with 37 MBq (1 mCi) 17-^{11}C-HDA (B). Quantitative analysis revealed no significant differences in rates of fatty acid utilization between the 2 tracers. RV = right ventricle; LV = left ventricle.

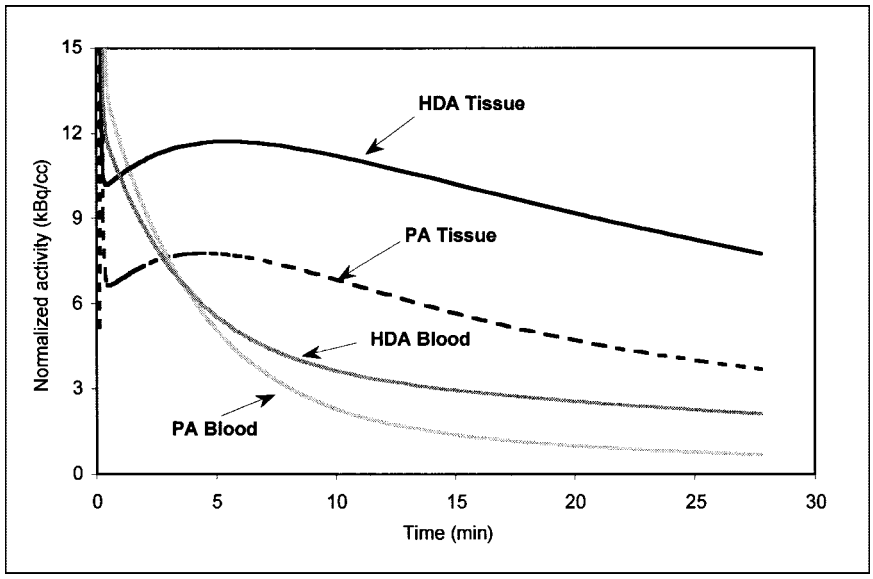

FIGURE 4. Time–activity curves from representative control dog. PA = 1-^{11}C-palmitate; HDA = 17-^{11}C-HDA. Activity shown is normalized for amount of activity injected and for weight of animal. Utilization of fatty acids was not significantly different; however, as seen with other ω-labeled fatty acids, there is ~50% increase in activity in heart for ω-labeled fatty acid (HDA) compared with that of C-1 labeled fatty acid (PA).

fraction for 1-^{11}C-palmitate and 17-^{11}C-HDA was determined to be 24% ± 2% and 23% ± 3%, respectively.

Metabolite Analysis

Paired arterial and coronary sinus blood samples were drawn at 1, 5, 10, and 20 min after administration of tracer in the dog studies. The conversion to ^{11}C-CO_2 was significantly greater for 1-^{11}C-palmitate compared with 17-^{11}C-HDA (Table 3).

Metabolite studies performed on arterial samples taken at 1 and 10 min after injection of HDA were found to contain predominantly fatty acid with <0.5% of other labeled material detected. No attempt was made to differentiate between C-17 and other labeled fatty acids in the plasma samples because of the resolution of the TLC plate. At 10 min, there was also glutamate or aspartate observed in arterial samples (Fig. 5), which suggests that the product of β-oxidation of 17-^{11}C-HDA, 3-^{11}C-propionic acid, is converted enzymatically to succinate, which then enters the tricarboxylic acid cycle as an anaplerotic substrate.

DISCUSSION

The results of this study demonstrate that an ω-labeled fatty acid, 17-^{11}C-HDA, has excellent imaging characteristics and behaves as expected in isolated perfused rat hearts and in intact dogs. In both sets of animal studies, the efflux of HDA products is similar to that of 1-^{11}C-palmitate, although there is a slight delay in the production of labeled product in rat heart studies, and the initial uptake appears to be greater in intact dog studies. In a manner similar to that reported for the ω-labeled palmitate (*7*), it is unlikely that the uptake into the heart for 17-^{11}C-HDA is greater than that for 1-^{11}C-palmitate.

In the isolated perfused heart studies, retention of tracer was longer after administration of 17-^{11}C-HDA compared with that after administration of 1-^{11}C-palmitate. This is consistent with the additional β-oxidation cycle steps needed to break down 17-^{11}C-HDA to its end product. Because the hearts were perfused with nonrecirculating media, under constant flow, the longer retention observed

TABLE 1
Substrate Utilization and Hemodynamics During Control and Dobutamine Canine Studies

Parameter	1-^{11}C-PA scan		17-^{11}C-HDA scan	
	Normal	Dobutamine	Normal	Dobutamine
Fatty acid utilization (nmol/g · min)	72 ± 1	202 ± 181	89 ± 9	135 ± 51
Palmitate utilization (nmol/g · min)	25 ± 2	50 ± 9	33 ± 5	39 ± 11
Glucose utilization (nmol/g · min)	214 ± 11	305 ± 24	213 ± 86	0 ± 514
Lactate utilization (nmol/g · min)	179 ± 33	28 ± 19	161 ± 52	131 ± 42
Double product (mm Hg · beats per min)	2,403 ± 83	8,393 ± 346	3,283 ± 445	12,076 ± 68

1-^{11}C-PA = 1-^{11}C-palmitate.
Comparison of substrate utilization in canine studies obtained by direct arterial and coronary sinus samples. As expected, dobutamine increases cardiac work and metabolism.

TABLE 2
Comparison of Fatty Acid Utilization Values by Direct Measurement and PET Modeling Studies

	Measured directly (nmol/g · min)		PET modeled (nmol/g · min)	
Condition	1-^{11}C-PA	17-^{11}C-HDA	1-^{11}C-PA	17-^{11}C-HDA
Control	71 ± 1	89 ± 9	80 ± 9	82 ± 9
Dobutamine	202 ± 181	135 ± 51	421	354

1-^{11}C-PA = 1-^{11}C-palmitate.

for 17-^{11}C-HDA is not the result of recirculating metabolites.

In the canine studies, the PET images obtained after administration of 17-^{11}C-HDA were quite similar to those obtained after 1-^{11}C-palmitate. Because of the time lag for metabolism of 17-^{11}C-HDA, images of similar counts could be obtained with a lower amount of tracer. Initial uptake of 17-^{11}C-HDA also appears to be higher than that of 1-^{11}C-palmitate.

From the time–activity curves obtained, the 2 tracers show similar clearance. The breakdown of HDA to metabolites such as labeled amino acids, observed in plasma at 10 min after administration, may also contribute slightly to reuptake in the myocardium. However, in dogs studied under the control state, the magnitude of this conversion is quite small and would not be expected to markedly effect calculations of the input function. This interpretation is substantiated by the ability to quantify fatty acid utilization

TABLE 3
Metabolite Analysis of ^{11}C Fatty Acids

	1-^{11}C-PA (%)		17-^{11}C-HDA (%)	
	Arterial	Coronary sinus	Arterial	Coronary sinus
Time	Normal			
1	96 ± 1	96 ± 1	97 ± 1	99 ± 1
5	94 ± 2	77 ± 2	97 ± 1	98 ± 3
10	89 ± 1	46 ± 3	97 ± 1	89 ± 2
20	65 ± 11	47 ± 11	92 ± 10	65 ± 14
	Dobutamine			
1	90	85	92	91
5	89	62	88	75
10	80	47	83	59
20	69	41	76	55

1-^{11}C-PA = 1-^{11}C-palmitate.
Percentage of radiotracer is amount of radioactivity remaining after acidification of sodium bicarbonate sample and sparging with nitrogen gas divided by total amount of radioactivity in equal-sized sample. All blood samples were corrected for decay and normalized to 1 g of blood.

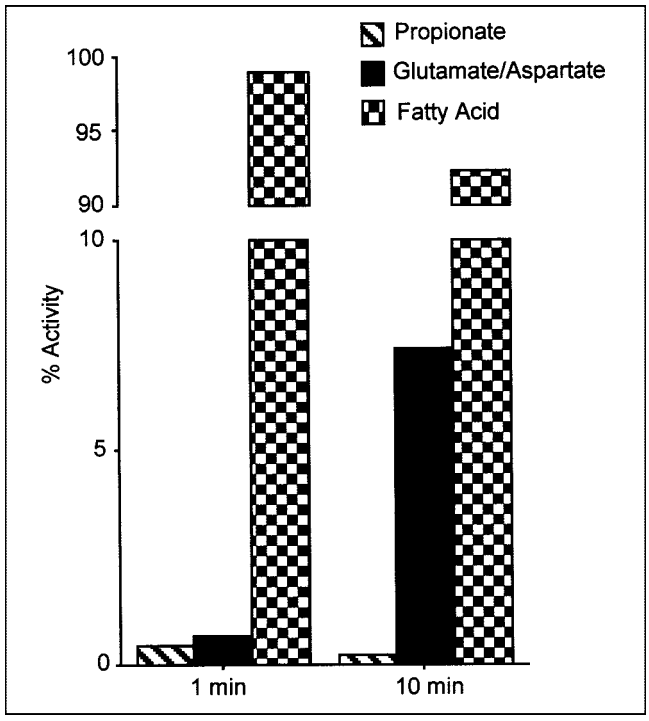

FIGURE 5. TLC comparison of metabolites in arterial plasma at 1 and 10 min after injection of 17-^{11}C-HDA. Because of TLC system used, aspartate and glutamate cannot be distinguished, but there was significant increase in labeled amino acids over time course of experiment. Major band in region of 17-^{11}C-HDA was collected, and no attempt was made to distinguish between 17-^{11}C-HDA and lower fatty acids on TLC.

with HDA (Table 2). The values for substrate utilization are somewhat higher than those reported (*13*); however, the trends between the normal and dobutamine-treated animals were similar. The error in all values is high because of the small number of animals studied.

It should be recognized, however, that the metabolic fate of the label in the 2 tracers is different. 1-^{11}C-Palmitate is oxidized to ^{11}C-CO_2 and only 1 cycle of β-oxidation is needed for the removal of the radiolabel. For 17-^{11}C-HDA, 7 sequential 2-carbon β-oxidation steps are required, and the result is a 3-carbon fragment, 3-^{11}C-propionic acid. The ultimate fate of 3-^{11}C-propionic acid is different from that of 1-^{11}C-acetate (the end product of the first β-oxidation cycle of 1-^{11}C-palmitate) on entering the tricarboxylic acid cycle. Sherry et al. (*17*) have demonstrated the fate of 3-^{13}C-propionic acid by NMR and showed that there is an enrichment in the 3-carbon of lactate, alanine, and aspartate. Because the metabolism of the 3-^{11}C-propionic acid should be identical, it will result in 2-^{11}C-succinic acid. The succinate CoA formed will then enter the tricarboxylic cycle as an anaplerotic substance and, because of the position of the label, the radiolabel will be removed as amino acids. The increased β-oxidation cycle time as well as the incorporation into amino acids accounts for the prolonged retention of tracer. Metabolic analysis of arterial plasma supports this

interpretation because there was an increase in labeled amino acids over the first 10 min, although labeled fatty acid in arterial blood still accounted for >90% of label in arterial blood at 10 min.

CONCLUSION

The results demonstrate that imaging with 17-^{11}C-HDA produces excellent quality images of the heart. Although the uptake and retention of 17-^{11}C-HDA are increased compared with that of 1-^{11}C-palmitate, modeling of the uptake of 17-^{11}C-HDA resulted in similar values compared with 1-^{11}C-palmitate and suggests that 17-^{11}C-HDA may be useful for evaluating fatty acid metabolism in subjects with MCAD and SCAD disorders.

ACKNOWLEDGMENTS

The authors thank Soliman Bakr for determination of fatty acid concentrations in plasma, Dr. Susan Chou for PET analysis, Chitra Manoj for assistance in operating the PET scanner, and Kristine M. Kulage for her assistance in preparing this manuscript. The authors also thank PETNET (New York, NY) and Mr. Michael Sanfillipo for allowing access to the cyclotron facilities to perform these experiments. This work was supported in part by a grant from the Department of Energy (grant DE-FG02-97ER62433) and the American Heart Association (grant 0040152N).

REFERENCES

1. Wanders RJ, Vreken P, den Boer ME, Wijburg FA, van Gennip AH, IJlst L. Disorders of mitochondrial fatty acyl-CoA beta-oxidation. *J Inherit Metab Dis.* 1999;22:442–487.
2. Roe CR, Wiltse HE, Sweetman L, Alvarado LL. Death caused by perioperative fasting and sedation in a child with unrecognized very long chain acyl-coenzyme A dehydrogenase deficiency. *J Pediatr.* 2000;136:397–399.
3. Scholte HR, Van Coster RN, de Jonge PC, et al. Myopathy in very-long-chain acyl-CoA dehydrogenase deficiency: clinical and biochemical differences with the fatal cardiac phenotype. *Neuromuscul Disord.* 1999;9:313–319.
4. Tein I. Metabolic myopathies. *Semin Pediatr Neurol.* 1996;3:59–98.
5. Bergmann SR, Herrero P, Sciacca RR, et al. Characterization of altered myocardial fatty acid metabolism in patients with inherited cardiomyopathy. *J Inherit Metab Dis.* 2001;24:657–674.
6. Kelly DP, Strauss AW. Inherited cardiomyopathies. *N Engl J Med.* 1994;330:913–919.
7. Buckman BO, VanBrocklin HF, Dence CS, Bergmann SR, Welch MJ, Katzenellenbogen JA. Synthesis and tissue biodistribution of [ω-^{11}C]palmitic acid: a novel PET imaging agent for cardiac fatty acid metabolism. *J Med Chem.* 1994;37:2481–2485.
8. Bergmann SR, Clark RE, Sobel BE. An improved isolated heart preparation for external assessment of myocardial metabolism. *Am J Physiol.* 1979;236:H644–H661.
9. Ramasamy R, Hwang YC, Whang J, Bergmann SR. Protection of ischemic hearts by high glucose is mediated, in part, by GLUT-4. *Am J Physiol Heart Circ Physiol.* 2001;281:H290–H297.
10. Hale SL, Alker KJ, Kloner RA. Evaluation of nonradioactive, colored microspheres for measurement of regional myocardial blood flow in dogs. *Circulation.* 1988;78:428–434.
11. Hodeige D, de Pauw M, Eechaute W, Weyne J, Heyndrickx GR. On the validity of blood flow measurement using colored microspheres. *Am J Physiol.* 1999;276:H1150–H1158.
12. Spinks TJ, Guzzardi R, Bellina CR. Performance characteristics of a whole-body positron tomograph. *J Nucl Med.* 1988;29:1833–1841.
13. Bergmann SR, Weinheimer CJ, Markham J, Herrero P. Quantitation of myocardial fatty acid metabolism using PET. *J Nucl Med.* 1996;37:1723–1730.
14. Welch MJ, Dense CS, Marshall DR, Kilborn MR. Remote system for production of carbon-11-labeled palmitate. *J Labelled Compds Radiopharm.* 1983;20:1087–1095.
15. Hostetler ED, Fallis S, McCarthy TJ, Welch MJ, Katzenellenbogen JA. Improved methods for the synthesis of [ω-^{11}C]palmitic acid. *J Org Chem.* 1998;63:1348–1351.
16. Långström B, Antoni G, Gullberg P, et al. Synthesis of L- and D-[methyl-^{11}C]methionine. *J Nucl Med.* 1987;28:1037–1040.
17. Sherry AD, Sumegi B, Miller B, et al. Orientation-conserved transfer of symmetric Krebs cycle intermediates in mammalian tissue. *Biochemistry.* 1994;33:6268–6275.

JNM The Journal of NUCLEAR MEDICINE

Synthesis and Initial Evaluation of 17-^{11}C-Heptadecanoic Acid for Measurement of Myocardial Fatty Acid Metabolism

T. Lee Collier, Yuying Hwang, Ravichandran Ramasamy, Robert R. Sciacca, Kathleen T. Hickey, Norman R. Simpson and Steven R. Bergmann

J Nucl Med. 2002;43:1707-1714.

The Journal of Nuclear Medicine is published monthly.
SNMMI | Society of Nuclear Medicine and Molecular Imaging
1850 Samuel Morse Drive, Reston, VA 20190.
(Print ISSN: 0161-5505, Online ISSN: 2159-662X)

SNMMI SOCIETY OF NUCLEAR MEDICINE AND MOLECULAR IMAGING